Antiband instability on vicinal Si(111) under the condition of diffusion-limited sublimation

V. Usov,[1,2] S. Stoyanov,[3] C. O Coileain,[1,2] O. Toktarbaiuly,[1,2] and I. V. Shvets[1,2]

[1]*School of Physics, Trinity College Dublin, Dublin 2, Ireland*
[2]*Centre for Research on Adaptive Nanostructures and Nanodevices (CRANN), Trinity College Dublin, Dublin 2, Ireland*
[3]*Department of Phase Transitions and Crystal Growth, Institute of Physical Chemistry, Bulgarian Academy of Sciences, 1113 Sofia, Bulgaria*

In this paper, we investigate the antiband instability on vicinal Si(111) surfaces with different angles of misorientation. It is known that prolonged direct current–annealing of Si(111) results in the formation of antibands; i.e., the step bunches with the opposite slope to the primary bunches. We provide a theoretical description of antiband formation via the evolution of the atomic steps' shape. We also derive a criterion for the onset of the antiband instability under the conditions of sublimation controlled by slow adatom surface diffusion. We examine this criterion experimentally by studying the initial stage of the antiband formation at a constant temperature of $1270\,^\circ$C while systematically varying the applied electromigration field. The experiment strongly supports the validity of the derived theoretical criterion and indicates the importance of accounting for the factor of critical field in the theoretical modeling of step bunching or antiband instabilities. Deduced from the comparison of theory and experiment, the Si surface atoms' effective charge cannot exceed double the elementary charge, set by the lower limit of kinetic characteristic length $d_s = 0.3$ nm. Using $d_s = 1.7 - 4.5$ nm draws values of the effective charge in line with the values reported in earlier studies.

I. INTRODUCTION

The step bunching instability on Si vicinal surfaces has long been a subject of scientific attention due to its complex temperature and electric current orientation dependencies.[1–10] When Si(111) is annealed by direct current (dc) driven along the miscut direction, adatom surface electromigration causes the atomic steps to gather together and creates step bunches separated by wide terraces. These step bunches grow with time and reach tens to hundreds of nanometers in height, while the terraces between them can grow to several micrometers in width.[1,2,10] Soon after the discovery of step bunching, it was found that prolonged dc annealing of Si(111) allows the surface morphology to further develop, giving rise to new morphologies such as antibands, which can be described as step bunches with slopes of the opposite sign as compared to the primary bunches.[11] Antibands are primarily formed via the shape evolution of atomic steps crossing the wide terraces between step bunches. At a certain stage of their development, these crossing steps acquire an S-shape, which does not manifest self-similarity when the terrace grows wider; i.e., beyond a certain terrace width, these S-shaped steps lose their stability and further develop towards a less symmetric shape.

The current theoretical model of the evolution of crossing steps towards the formation of antibands considers the down-step adatom electromigration and is derived for the case of the attachment-detachment–limited regime (or step kinetics–limited regime).[12] In this regime, surface sublimation is controlled by the atomic processes at elementary steps because the rate of adatom attachment-detachment is much slower than the rate of adatom surface diffusion. This results in a pile-up of adatoms at the step edges and creates the gradient of their concentration across large terraces separating step bunches. This nonuniformity of the adatom concentration eventually breaks the stability of the S-shape of crossing steps and initiates the process of antiband formation. However, initially, this gradient in adatom concentration can be balanced by the variation of chemical potential μ_s along the crossing steps, which is given by $\mu_s = -\bar{\beta} b^2 C_s$, where $\bar{\beta}$ is the step stiffness, b is atomic spacing, and C_s is the step curvature.[12] Therefore, the appropriate variation of the step curvature C_s can compensate for the nonuniformity of the adatom concentration across the terrace and stabilize the steady-state S-shape of the crossing steps. This compensation mechanism fails as the terrace width grows, initiating the onset of the antiband instability, which occurs when the terrace width (L_t) satisfies the necessary condition:[12]

$$\frac{F L_t^2}{\bar{\beta} b^2} > 2, \tag{1}$$

where F, given by $F = q_{ef} E$, is the electromigration force acting on adatoms, E is the electric field applied across the sample, and q_{ef} is the effective electric charge of surface adatoms. The remarkable aspect of the condition (Eq. (1)) is that it does not account for the degree of surface vicinality in any form. It implies that for a given force F, the terrace width L_t required for the onset of the antiband instability is the same for any initial interstep distance (l), which is determined by the overall surface off cut from the low index plane.

The results of recent experimental investigations strongly suggest that sublimation on the Si(111) surface is a diffusion-limited process,[13–15] which is characterized by relatively slow surface adatom diffusion and fast kinetics at the atomic steps. Here, we provide a theoretical treatment of the antiband instability under the condition of diffusion-limited sublimation. We also experimentally study the onset of this instability and compare experimental and theoretical findings.

II. THEORY OF STEP SHAPE INSTABILITY AND ANTIBAND FORMATION

Depending on temperature, the step bunching process on Si(111) can be maintained by either up-step–or down-step–

driven dc current (e.g., in the temperature regimes 1050–1240 or 1250–1350 °C, respectively).[6,16] Recent experimental studies have affirmed that in both annealing regimes, antibands are located close to lower step bunches, while in the case of the attachment-limited sublimation, they are expected to grow closer to the upper step bunch when the heating current is driven in the up-step direction.[17] This was explained by a possible change in sign of surface adatoms' effective charge from positive at higher temperatures to negative at lower.[10,18] However, the assumption of a sign change is in contradiction with the results of earlier experimental studies, which clearly demonstrated that adatom electromigration on Si(111) proceeds in the direction of the applied electric field over a wide range of temperatures.[19]

In this section, we derive an expression for the adatom concentration gradient under the conditions of slow surface adatom diffusion and show that this gradient is independent of the direction of the electric current. As a consequence, the location of antibands under these conditions is no longer expected to change upon reversal of the electric current direction, which is in agreement with the experimental observations.[11,17] The expression for the gradient is later used to derive the condition for the onset of the antiband instability.

A. Nonuniformity of the adatom concentration in the case of surface diffusion-limited sublimation

The adatom concentration gradient on wide terraces between step bunches is induced by two rather different mechanisms in the two aforementioned regimes. In the step kinetics–limited regime, the concentration gradient is induced directly by the electromigration force F, which pushes adatoms towards the atomic step at the terrace's edge, where the adatoms create a "pile" due to the slow rate of the attachment process.[12] In contrast, the adatom concentration at the step on the opposite side of the terrace is lowered, because atoms detached from the step are immediately removed by means of electromigration.

In the diffusion-limited regime, the concentration gradient is created by a different mechanism, which is related to the repulsion interaction between atomic steps. On the macroscopic level, this mechanism is based on the dependence of the local chemical potential on the curvature of the crystal surface. The positive surface curvature on one side of a wide terrace and negative surface curvature on the other side create conditions for the existence of the concentration gradient. The gradient created in this way can be neglected in the case of the attachment-limited sublimation since its contribution is not significant compared to the direct contribution of electromigration force.[12] However, in the diffusion-limited regime, the intensive atom exchange between the crystal phase and the adlayer of adatoms results in nearly equilibrium adatom concentration in the vicinity of the jth step, which is given by:[4]

$$n_s^e(x_j) = n_s^e \left[1 + \tilde{A} \left(\frac{1}{l_{j-1}^3} - \frac{1}{l_j^3} \right) \right], \qquad (2)$$

where $\tilde{A} = \frac{2\Omega g}{kT}$, n_s^e is the equilibrium adatom concentration on an ideal vicinal surface where $l_{j-1} = l_j$, g is the strength

of the entropic and stress-mediated repulsion between atomic steps, Ω is the area of a single atomic site, and $l_j = x_{j+1} - x_j$ is the width of the jth terrace between atomic steps with the coordinates x_j and x_{j+1}. When the jth terrace is the large terrace between two bunches (i.e., $l_j = L_t$), the condition $L_t \gg l_{j-1} \sim l_{j+1}$ can be applied, and the expressions for $n_s^e(x_j)$ and $n_s^e(x_{j+1})$ can be simplified by neglecting the term $\frac{1}{L_t^3}$, giving:

$$n_s^e(x_j) = n_s^e \left[1 + \tilde{A} \left(\frac{1}{l_{j-1}^3} \right) \right]$$

and

$$n_s^e(x_{j+1}) = n_s^e \left[1 - \tilde{A} \left(\frac{1}{l_{j+1}^3} \right) \right]. \qquad (3)$$

Making use of Eq. (3), one obtains the expression for the adatom concentration gradient G_r on a wide terrace:

$$G_r = \frac{n_s^e(x_j) - n_s^e(x_{j-1})}{L_t} = \frac{1}{L_t} n_s^e \tilde{A} \left[\frac{1}{l_{j-1}^3} + \frac{1}{l_{j+1}^3} \right], \qquad (4)$$

where l_{j-1} is the width of the highest terrace in the lower bunch (outflow region where atomic steps detach from the bunch), and l_{j+1} is the width of the lowest terrace of the higher bunch (inflow region).

Expressions for l_{j+1} and l_{j-1} were derived in earlier theoretical studies (Eq. (22) in Ref. (20)) for a conserved system where surface desorption could be neglected.[20] It should be noted that l_{j+1} and l_{j-1} behave differently in the case of non-negligible desorption, as was revealed by numerical integration of step motion equations within the framework of one-dimensional model.[3] These numerical calculations of l_{j+1} reproduce the result obtained for a conserved system[20] but give considerably larger values of l_{j-1}. As an approximation, we will use the expression derived for a conserved system[20] but written with somewhat different notation:

$$l_{j-1} = l_{j+1} = \left(\frac{2\Omega g}{|F| d_s} \right)^{1/3} N^{-1/3}, \qquad (5)$$

where $d_s = \frac{D_s}{K}$ is the kinetic characteristic length, D_s is the coefficient of surface diffusion, K is the step kinetic coefficient, g is the step repulsion coefficient, and N is the number of steps in the bunch, which in the following considerations is assumed to be the same for all bunches. Substituting Eq. (5) into Eq. (4) gives an expression for the adatom concentration gradient:

$$G_r = -2n_s^e \frac{N}{L_t} \left(\frac{|F| d_s}{kT} \right). \qquad (6)$$

Equation (6) suggests that, in the regime characterized by the slow surface diffusion, the gradient of the adatom concentration across wide terraces indirectly arises through the presence of large adjoining step bunches on the terraces' sides. The applied electric field results in the formation and subsequent growth of the step bunches, which provide conditions for the creation of the concentration gradient. The essential aspect of Eq. (6) is that the adatom gradient depends on the absolute value of the electromigration force and is independent of its direction.
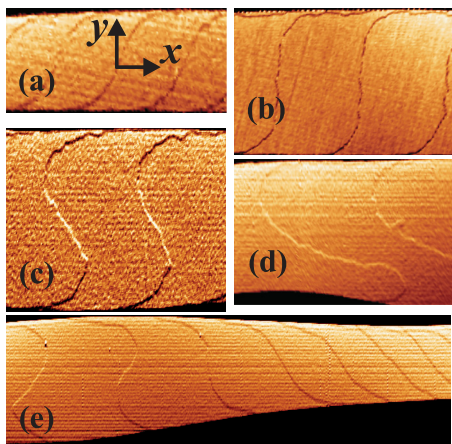
FIG. 1. (Color online) Evolution of crossing steps' shape towards the formation of antibands on Si(111) terraces. (a) Crossing steps are curved in the long S-shape. The sign of the step's slope remains the same along the entire step. (b) Crossing steps are aligned perpendicular to the step bunches. A further increase in the terrace width allows the transition to the S-shape. (c) Crossing steps in the steady-state S-shape, characterized by change in sign of the slope in each half of the terrace. (d) Crossing steps gradually develop a segment with a zero slope, indicating the onset of the antiband instability. (e) Crossing steps "frozen" at different stages of their evolution on a single widening terrace.

B. Shape of the crossing steps—limits of stability

For simplicity, the shapes of crossing steps are analyzed for the down-step electromigration under equilibrium conditions. Under equilibrium conditions, the surface desorption is either negligible or compensated by the appropriate deposition,[17] and the crossing steps remain in their fixed positions. In the following, we will consider the coordinate system with the x axis along the step bunches and the y axis normal to them, with the positive direction from the lower to the higher terraces and the origin in the middle of the terrace (Fig. 1(a)). Using the same approach as formulated by Thurmer,[12] the adatom concentration gradient (G_r) compensation by the variation of the step curvature C_s can be expressed in these coordinates as

$$\bar{\beta} n_s^e \mathbf{\Omega} C_s = G_r y. \tag{7}$$

The crossing steps' equilibrium shape $y(x)$ can be found by solving differential Eq. (7), which is equivalent to

$$\frac{y''}{(1 + y'^2)^{3/2}} = ay \tag{8}$$

with $a = \frac{G_r kT}{\bar{\beta} n_s^e \mathbf{\Omega}}$, and can be easily reduced to

$$y' = \pm \frac{1}{ay^2 - C} \sqrt{4 - (ay^2 - C)^2}, \tag{9}$$

where C is an arbitrary constant that can be found by applying the boundary condition $y'(\frac{L_t}{2}) = 0$:

$$C = 2 + a \left(\frac{L_t}{2} \right)^2. \tag{10}$$

Equations (9) and (10) provide a background for clear understanding of the different stages of the crossing steps'

evolution and transitions between these stages. Initially, the crossing steps are curved in the long S-shape, and the sign of their slope $y' = \frac{dy}{dx}$ remains the same over the y-interval given by $0 \leqslant y \leqslant \frac{L_t}{2}$ (Fig. 1(a)). This situation is realized when L_t satisfies the inequality:

$$L_t < 2 \sqrt{\frac{2}{|a|}}, \tag{11}$$

leading to the equation for the critical value of terrace width L_{tcr}:

$$L_{tcr} = 2 \sqrt{\frac{2\bar{\beta} n_s^e \mathbf{\Omega}}{|G_r| kT}}. \tag{12}$$

Once L_t exceeds L_{tcr}, the crossing steps make the transition from the long S-shape (Fig. 1(a)) to the S-shape (Fig. 1(b) and 1(c)). The S-shape is characterized by a change in sign of the slope in each half of the terrace and can only be maintained in the limited interval of L_t values. The lower boundary of this interval is determined by L_{tcr}, while the upper limit $L_{t\,max}$ can be determined from the condition $y'(0) = 0$:

$$L_{t\,max} = 4 \sqrt{\frac{\bar{\beta} n_s^e \mathbf{\Omega}}{|G_r| kT}}. \tag{13}$$

For $L_t > L_{tmax}$, the step's slope becomes zero in the middle of the terrace, and the equilibrium S-shape can no longer exist. At this point, the variation of step curvature cannot compensate for the gradient of the adatom concentration, so that the steps lose their stability and gradually lose their symmetry, marking the onset of the antiband instability (Fig. 1(d) and 1(f)).

These results are valid for the equilibrium shape of crossing steps but cannot be applied directly to high-temperature regimes where sublimation rates can be significant (e.g., $1250 < T < 1350\,^\circ$C). As a result, the steps do not retain their positions on terraces but move along at a measurable rate. In this case, one should consider the steady state of crossing steps, which needs some comments. Generally, the shape evolution of a moving step is described by equations:[21]

$$\frac{\partial x}{\partial t} = -V \sin\varphi + \frac{dV}{d\varphi} \cos\varphi, \quad \frac{\partial y}{\partial t} = V \cos\varphi + \frac{dV}{d\varphi} \sin\varphi, \tag{14}$$

where $x(\varphi,t)$ and $y(\varphi,t)$ are coordinates of a point on the step, φ is the angle between the normal to the step at this point and the x axis, t is the sublimation time, and V is the step velocity given by

$$V = K\mathbf{\Omega}(n_s - n_s^e). \tag{15}$$

The $V(\varphi)$ dependence is quite complex because the step kinetic coefficient K is generally anisotropic. This anisotropy is created by kinks produced along the step by geometrical misalignment of the step orientation and the crystallographic directions for atomically straight steps. When the density of these kinks exceeds the density of thermally activated kinks, the coefficient K becomes a function of φ. Also, V depends on φ via the adatom undersaturation (or oversaturation) $\Delta n_s = n_s - n_s^e$, because the adatom concentration n_s in Eq. (15) has a gradient along the y axis, while the equilibrium concentration

n_s^e depends on the step curvature, which varies along the step, or, in other words, it depends on $x(\varphi,t)$ and $y(\varphi,t)$.

Such complex $V(\varphi)$ dependence makes calculating the time evolution of crossing steps a challenging task. However, here we are interested in the relatively simple case of the steady-state shape, where the step motion is limited to simple translation along the x axis and Eq. (14) can be reduced to:

$$\frac{\partial x}{\partial t} = -V_{tr}, \quad \frac{\partial y}{\partial t} = 0, \tag{16}$$

where V_{tr} is the velocity of the step's translational motion as a whole. Finally, combining Eqs. (15) and (16) results in the equation for the steady-state shape of the crossing step:

$$y'' = ay(1 + y'^2)^{3/2} + \frac{V_{tr}}{\Omega K} a'(1 + y'^2) + \Delta n_s a'(1 + y'^2)^{3/2}, \tag{17}$$

where

$$a' = \frac{kT}{\bar{\beta} n_s^e \Omega}. \tag{18}$$

Equation (17), which takes into account the undersaturation Δn_s and the translational velocity V_{tr}, can be reduced to Eq. (8), derived for the equilibrium conditions, by assuming that Δn_s and V_{tr} are negligible. However, in the general case, the undersaturation and its influence on the step velocity will result in a deviation of crossing steps from their equilibrium shape and affect the final form of Eqs. (12) and (13) for L_{tcr} and $L_{t\,max}$.

C. Onset of antiband formation under conditions of diffusion-limited sublimation

Equation (6) for the gradient in the adatom concentration can be modified by taking into account that the number of steps in the bunch is given by $N = \frac{L_t + L_{bunch}}{l}$ and substituting this expression into Eq. (6), which results in:

$$G_r = -2n_s^e \frac{1}{l} \left(1 + \frac{L_{bunch}}{L_t}\right) \left(\frac{|F|\,d_s}{kT}\right), \tag{19}$$

where L_{bunch} is the width of the step bunch, and l is the mean initial terrace width. As was discussed earlier, the formation of antibands begins when crossing steps develop segments aligned parallel to the step bunches after the terrace width L_t exceeds L_{tmax}, given by Eq. (13). Substituting Eq. (19) into Eq. (13) results in the criterion for the onset of the antiband instability under conditions of slow surface adatom diffusion:

$$L_t^2 \left(1 + \frac{L_{bunch}}{L_t}\right) \frac{d_s|F|}{\bar{\beta}\,l\,\Omega} \geqslant 8. \tag{20}$$

The condition $L_{bunch} \ll L_t$ can be applied in the case of a low vicinal surface, and the inequality Eq. (20) can be simplified to:

$$L_t^2 \frac{d_s|F|}{\bar{\beta}\,l\,\Omega} \geqslant 8, \tag{21}$$

which is similar to Eq. (1). The relationships in Eqs. (20) and (21) contain the ratio $\frac{d_s}{l}$, which is determined by the surface miscut from the low index crystallographic plane. This is in striking contrast with Eq. (1), which was derived for the case of attachment-limited sublimation[12] and does not account for the degree of surface vicinality in any form.

It is important to point out that Eq. (20) was obtained by solving Eq. (8), which describes the equilibrium shape of crossing steps. It captures the essential thermodynamic aspect of the problem, while the process of antiband formation can be substantially more complex when investigated experimentally. As was discussed earlier, a more accurate result can be obtained by solving Eq. (17), which describes the steady-state shape of crossing steps and accounts for the kinetic processes and undersaturation at the steps. However, the solution of Eq. (17) is currently unknown to us.

III. EXPERIMENTAL STUDY OF THE EFFECTS OF SURFACE VICINALITY ON THE FORMATION OF ANTIBANDS

The condition in Eq. (20) formulated in the form of an inequality suggests that L_t and L_{bunch} must reach certain minimum widths for any fixed values of l and F in order to achieve the onset of antibands. F can be controlled in experiments by varying the electric field applied across the sample, while l can be set out by slicing a low index surface at an appropriate angle α. In the next section, we experimentally examine Eq. (20) by studying the relationships among the onset of the antiband instability, the electromigration field, initial distance between the atomic steps, and the width of step bunches and terraces.

A. Experimental procedure

We examined the onset of the antiband instability on Si(111) using a vacuum setup with a base pressure of 2 $\times$ 10^{-10} Torr, which combines independently controlled dc current and irradiative heating.[22] The radiative heating was supplied by an empty crucible of an effusion cell surrounding a custom-made dc-annealing stage. The sample temperature was extracted from the sample resistance, essentially using the sample as a resistance thermometer. The capacity to decouple the dc current from the sample temperature enabled us to control the strength of the electric field while maintaining the sample at a desired temperature. The strongest electric field $E = 3.6$ V/cm was applied when the dc current was the only source of heating. The weakest field was determined by the critical electromigration field (E_{cr}), i.e., the minimum electric field required to initiate the step bunching process.[13]

Samples were diced in the shape of rectangular 20 $\times$ 1.3 mm^2 strips from n-type doped 0.525-mm-thick Si(111) wafers, with the misorientation angles (α) from the Si(111) plane in the range $1.1°-4°$ towards the [11-2] direction, and the long sides of the samples aligned to the miscut direction. Initially, each sample was outgassed in a crucible for 24 hours at 700 °C. To reduce surface defects, the samples were then dc-annealed for 24 hours at a temperature of approximately 450–500 °C, which was followed by repeated dc flash-annealing up to 1250 °C for 10 seconds. Samples were later annealed for time intervals ranging between 15 and 60 minutes at 1270 °C (regime III) with current driven along the miscut in the down-step direction. At

this temperature, the Si(111) surface bunches at the high rate of approximately 1 step/second[23] and reaches the phase of antiband formation relatively rapidly, compared to other temperature intervals. Normally, two samples of the same miscut were annealed with the same electric field to confirm consistency of the results. Shorter annealing times were used for samples annealed with stronger electric fields.

Prolonged sample annealing in a vacuum can result in carbon segregation. Therefore, a separate experiment was set up in order to investigate the extent of surface contamination that could be potentially induced by the described annealing procedure. Auger electron spectroscopy analysis showed that after flash annealing to 1250 °C, the surface was free from carbon and oxygen contamination and remained clean after further annealing for 2 hours at 1270 °C.[22] After the annealing sequence, the samples were maintained at 650 °C for an hour using only irradiative heating. Finally, the samples were removed from vacuum, and the surfaces were analyzed *ex situ* using atomic force microscopy (AFM).

B. Experimental results and discussion

The surface morphology created on Si(111) by extended annealing was characterized by step bunches separated by several-micrometer-wide terraces. It was important to analyze only terrace segments that featured crossing steps at the same stage of their evolution. Therefore, the annealing times were adjusted for all samples so as to create a large selection of terraces comprising crossing steps in the same symmetric steady-state S-shape such as in Fig. 1(c). Significant variation in the size of these terraces was observed, with some being up to 80% wider than the detected minimum. Qualitatively, this is in agreement with the inequality in Eq. (20), which gives a necessary but insufficient condition for the onset of the antiband instability. Thus, for fixed values of F and l, the lower limit of this relationship is defined by the widths of the terrace and the corresponding step bunch, which provide the lowest value of the product $L_t^2(1 + \frac{L_{bunch}}{L_t})$, denoted as L_m from now on. As expected, the terraces of the least width were found to be adjoined to the proportionally narrowest step bunches throughout the entire experiment.

Figure 2(a) shows the dependence of the ratio (l/L_m) on the electromigration field E for the terrace segments containing crossing steps in the symmetric steady-state shape. For each experimental point in the figure, 20–25 sites of 50 × 50 μm^2 were randomly selected across the entire step bunched area, and the L_m value was drawn from 30–40 separate terraces containing crossing steps in the steady-state S-shape. The critical field is known to be weaker for Si(111) with lower vicinality, and therefore samples with lower angles of misorientation provided a wider range of electric fields over which the antiband instability could be studied.

The open circles in Fig. 2(a) represent the $E(l/L_m)$ dependence for the narrowest terrace segments featuring crossing steps aligned perpendicular to the step bunches as in Fig. 1(b). These terraces can be deemed to have reached their critical size L_{tcr} given by Eq. (12) as a further increase in the terrace width allows the transition to the S-shape where the crossing steps are separated into two distinct lobes (Fig. 1(c)). This graph was
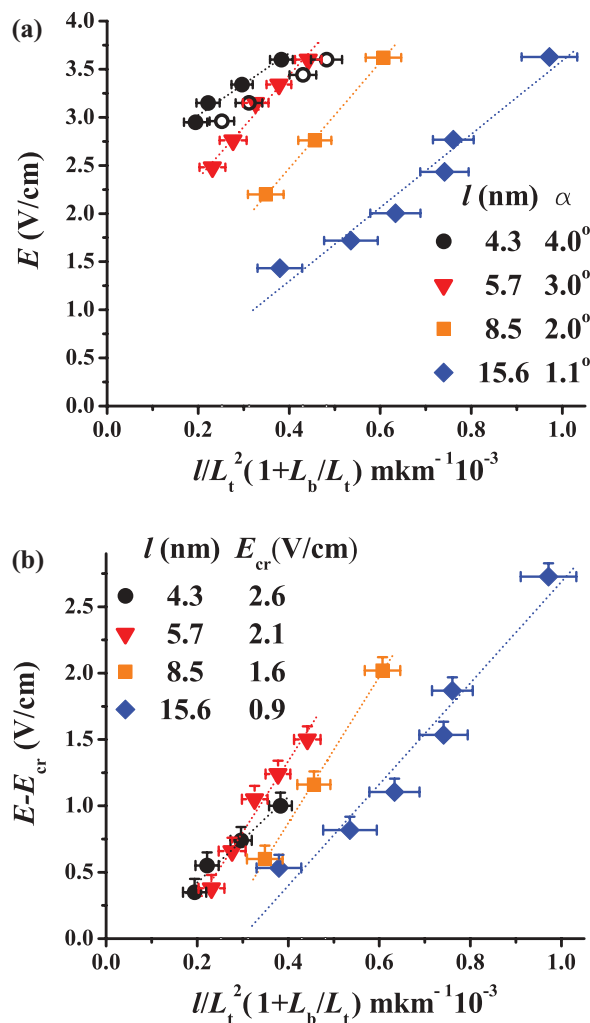

FIG. 2. (Color online) (a) Applied electric field E plotted as a function of the highest value of the product $\frac{l}{L_t^2(1+L_{bunch}/L_t)}$ for Si(111) with different mean initial terrace width l. L_t and L_{bunch} denote the width of the terrace and the adjoining step bunch, respectively. The plot is expected to produce a straight line according to Eq. (20). Only terraces containing crossing steps in the symmetric S-shape were taken into account. α indicates the angle of misorientation from the Si(111) surface towards the [11-2] direction. (b) The electric field in Fig. 2(a) is replaced by $E - E_{cr}$, where E_{cr} is critical field, i.e., the lowest field required to initiate the step bunching process.

plotted for Si(111) with a 4° misorientation and shows merely an offset in the position of L_m when compared to the graph obtained for terraces with the crossing steps in the steady-state shape. Thus, for the same initial interstep separation, the exponent in the $E(L_m)$ relationship is unaffected by the choice of the step's stage of evolution.

Figure 2(a) shows that the minimum terrace and bunch widths required for the onset of antiband instability progressively increase as the electric field is reduced. The $E(l/L_m)$ graphs are linear and clearly demonstrate that the terrace and bunch widths strongly depend on the initial distance between atomic steps l, in agreement with Eq. (20). Due to the nature of the experiment, the pairs of step bunches and terraces that provide the absolute minimum of the product

L_m could not be detected on every annealed surface, which can explain the observed difference in the slope between the graphs but cannot account for their significant offset along the E axis. However, this offset is not significant for Si(111) with $\alpha = 1.1°$ ($l = 15.6$ nm), and therefore the $E(l/L_\mathrm{m})$ dependence can be directly compared with Eq. (20), and the value of the effective charge can be estimated. Using the extrapolated value for $\bar{\beta} = 28$ meV/Å,[12,24,25] the lower limit of the characteristic length $d_\mathrm{s} = 0.3$ nm and $\Omega \approx 10^{-1}$ nm^2 gives a value of the effective charge $q_\mathrm{ef} = 1.95|e|$. However, $d_s = 1.7 - 4.5$ nm gives $q_\mathrm{ef} = (0.35 - 0.13)|e|$ as reported in earlier studies.[10,12,23] This indicates that there is a possibility for highly vicinal surfaces, with small l, to enter into a crossover between attachment-limited and diffusion-limited regimes where the characteristic length d_s is comparable to l. It should be mentioned here that it is the d_s value as compared to l that determines the regime of sublimation[26] and that Eq. (1) and Eq. (20) describe two limiting cases, given by conditions $d_s \gg l$ and $d_s \ll l$, respectively. For completeness, the $E(L_\mathrm{t})$ dependence for $\alpha = 1.1°$ was compared with Eq. (1) for the attachment-limited regime, and the value $q_\mathrm{ef} = 0.013|e|$ was found.

A possible explanation for the graph's offset along the E axis is that the $E(l/L_\mathrm{m})$ dependence does account for the relative proximity of the electromigration field E to the critical point, where the surface is stable to the step bunching. Equation (20) was also derived with the implicit assumption that E_cr equals zero, which is in disagreement with the results of the latest experimental investigations. These investigations demonstrate that, in the most studied third temperature regime, the critical field for Si(111) is significant and grows linearly with the increasing surface misorientation angle.[13] For example, for Si(111) with misorientation of 3° ($l = 5.7$ nm) or 4° ($l = 4.3$ nm), $E = 2.0$ V/cm is less than E_cr, and the value of L_m obtained with these parameters from Eq. (20) would not be physically meaningful.

For $E < E_\mathrm{cr}$, step bunching cannot be initiated, and wide terraces required for antiband formation cannot be created. This, however, is not reflected in Eq. (6), which predicts the presence of the gradient at any applied electric field. The reason for this disagreement can be found in Eq. (5), which is used in the derivation of Eq. (6). Equation (5) is valid only for a conserved system with negligible desorption, which assumes that the adatom's mean diffusion path λ_s tends to infinity.[27] As a result, the critical field tends to zero in accordance with the equation for E_cr,

$$|E_{cr}| = \frac{12\mathbf{\Omega} g}{d_s \lambda_s^2 q_\mathrm{eff} l}, \tag{22}$$

obtained under the conditions of slow adatom diffusion.[13] Therefore, when using Eq. (5), we implicitly assume that $E_\mathrm{cr} = 0$ and pass this assumption onto Eq. (20). This is a necessary measure since analytical expression for the width of the highest and lowest terraces in the bunch (Eq. (5)) is currently unavailable for the practical case of intensive sublimation.

In order to approximately account for the factor of critical field, E in Eq. (20) can be replaced by the difference $E - E_\mathrm{cr}$, and L_m can be plotted versus $E - E_\mathrm{cr}$ as shown in Fig. 2(b).

In this case, the graphs' offset along the E axis is significantly reduced, and experimental data collected on Si(111) with different misorientation partly overlap, as would be expected from Eq. (20). This indicates the importance of accounting for the critical field when modeling step bunching or antiband instabilities. This problem was not identified in earlier theoretical studies, where E_cr was implicitly assumed to be equal zero.[26] Extrapolating the $E_\mathrm{cr}(l)$ experimental dependence[13] shows that in the practical case of heavy desorption, this is a reasonable assumption for surfaces with a small angle of misorientation of less than 0.5°.

IV. CONCLUSIONS

We provided a theoretical treatment of the antiband instability under the condition of adatom surface diffusion-limited sublimation. Under this condition, we derived an expression for the adatom concentration gradient across the wide terraces where the antiband growth takes place. We showed that this gradient arises through the presence of step bunches separating terraces and depends on the absolute value of the electromigration force. Importantly, it is independent of the force direction, in strong agreement with the experiments on Si(111), where the antibands were found to be created in the same locations on terraces, regardless of whether the electric field was applied in the up-step or the down-step direction.

We analyzed the limits of stability of crossing steps' shape under equilibrium conditions and used the expression for the concentration gradient to derive the condition for the onset of the antiband instability. Remarkably, this condition implies that the terrace width required to achieve the formation of antibands strongly depends on the degree of surface vicinality; i.e., for a given strength of the applied electric field, wider terraces and step bunches are needed in order to create the antibands on the surfaces with wider initial interatomic-step distances (or lower angles of surface misorientation from the low index plane).

The condition was experimentally examined by studying an early stage of the antiband formation on the Si(111) surface with different misorientation angles from the Si(111) plane. The experiments were conducted at constant temperature of 1270 °C while systematically varying the applied electric field. This allowed us to investigate the relationships among the onset of the antiband instability, the electromigration field, initial distance between the atomic steps, and the width of step bunches and terraces. The experiment strongly supports the validity of the theoretically derived condition for the onset of the antiband instability. It also indicates the importance of accounting for the factor of critical field in the theoretical models of step bunching or antiband instabilities.

[1] A. Latyshev, A. Aseev, A. Krasilnikov, and S. Stenin, Surf. Sci. **213**, 157 (1989).

[2] V. Usov, C. O Coileain, and I. V. Shvets, Phys. Rev. B **83**, 155321 (2011).

[3] J. Krug, V. Tonchev, S. Stoyanov, and A. Pimpinelli, Phys. Rev. B **71**, 045412 (2005).

[4] S. Stoyanov, in *Nanophenomena at Surfaces*, edited by M. Michailov (Springer-Verlag, Berlin, 2011), Vol. 47 of Springer Series in Surface Sciences, p. 253.

[5] C. Misbah, O. Pierre-Louis, and Y. Saito, Rev. Mod. Phys. **82**, 981 (2010).

[6] F. Leroy, D. Karashanova, M. Dufay, J. M. Debierre, T. Frisch, J. J. Métois, and P. Müller, Surf. Sci. **603**, 507 (2009).

[7] W. Hong, Z. Suo, and Z. Zhang, J. Mech. Phys. Solids **56**, 267 (2008).

[8] Y. Yamada, A. Girard, H. Asaoka, H. Yamamoto, and S. I. Shamoto, Phys. Rev. B **76**, 153309 (2007).

[9] M. Dufay, T. Frisch, and J. M. Debierre, Phys. Rev. B **75**, 241304(R) (2007).

[10] K. Fujita, M. Ichikawa, and S. S. Stoyanov, Phys. Rev. B **60**, 16006 (1999).

[11] A. Latyshev, A. Krasilnikov, and A. Aseev, Surf. Sci. **311**, 395 (1994).

[12] K. Thürmer, D. J. Liu, E. D. Williams, and J. D. Weeks, Phys. Rev. Lett. **83**, 5531 (1999).

[13] C. O Coileain, V. Usov, I. V. Shvets, and S. S. Stoyanov, Phys. Rev. B **84**, 075318 (2011).

[14] B. J. Gibbons, S. Schaepe, and J. P. Pelz, Surf. Sci. **600**, 2417 (2006).

[15] K. L. Man, A. B. Pang, and M. S. Altman, Surf. Sci. **601**, 4669 (2007).

[16] A. Latyshev, A. Aseev, A. Krasilnikov, and S. Stenin, Surf. Sci. **227**, 24 (1990).

[17] E. E. Rodyakina, S. S. Kosolobov, and A. V. Latyshev, JETP Lett. **94**, 147 (2011).

[18] D. Kandel and E. Kaxiras, Phys. Rev. Lett. **76**, 1114 (1996).

[19] M. Degawa, H. Minoda, Y. Tanishiro, and K. Yagi, Surf. Sci. **461**, L528 (2000).

[20] M. Sato and M. Uwaha, Surf. Sci. **442**, 318 (1999).

[21] A. A. Chernov, *Modern Crystallography III: Crystal Growth. Part I* (Springer, New York, 1984).

[22] V. Usov, C. O Coileain, and I. V. Shvets, Phys. Rev. B **82**, 153301 (2010).

[23] Y. Homma and N. Aizawa, Phys. Rev. B **62**, 8323 (2000).

[24] K. Sudoh, T. Yoshinobu, H. Iwasaki, and E. D. Williams, Phys. Rev. Lett. **80**, 5152 (1998).

[25] J. M. Bermond, J. J. Metois, J. C. Heyraud, and F. Floret, Surf. Sci. **416**, 430 (1998).

[26] D. J. Liu and J. D. Weeks, Phys. Rev. B **57**, 14891 (1998).

[27] S. Stoyanov and V. Tonchev, Phys. Rev. B **58**, 1590 (1998).